JOURNAL OF GUIDANCE, CONTROL, AND DYNAMICS
Vol. 16, No. 3, May-June 1993

Guidance for an Aerocapture Maneuver

J. G. Gurley*
Hughes Aircraft Company, El Segundo, California 90009

Aerocapture, which has been described as "essential for cost-effective space transportation," imposes severe guidance and control problems. A closed-loop control law is formulated that provides stable control in the presence of reasonable errors in approach guidance and in knowledge of the atmospheric density profile. Navigational accuracy requirements can be satisfied by a combination of approach tracking and onboard inertial measurements, supplemented, in the case of a Mars encounter, by a radar altimeter or its functional equivalent.

I. Introduction

AEROCAPTURE—the use of aerodynamic forces to effect capture of an interplanetary vehicle into a satellite orbit about the destination planet—has been identified as a critical new technology with very great potential to reduce the cost of planetary exploration, especially robotic sample return missions and manned missions to Mars. NASA's "90-Day Study" describes aerobraking as "essential for cost-effective space transportation."[1] Although the technology needed for aerocapture is similar to that used for the return of spacecraft from orbit to Earth, as typified by Apollo and the Space Shuttle, it imposes much more severe demands on the thermal protection system, because of the greater energy dissipation, and on the guidance and control system, because of the very shallow entry angles used to reduce the maximum heating rates and aerodynamic forces.[2,3] This report describes an investigation into the guidance and control requirements and examines the robustness of a conceptual guidance and control scheme with respect to variability in the atmospheric parameters of the destination planet, the aerodynamic coefficients of the vehicle, and the type and quality of the guidance instrumentation.

II. Need for Active Guidance During an Aerocapture Maneuver

Aerocapture utilizes aerodynamic forces to capture, into a bound orbit, a spacecraft approaching a planet at hyperbolic velocity (Fig. 1). If lateral steering corrections are moderately small, then the principal features of the spacecraft motion can be represented by assuming a spherically symmetrical inverse-square gravitational force μ/r^2, neglecting atmospheric rotation, and considering only the inplane variables r (radial distance from the center of the planet), θ (phase angle in the plane of the trajectory), V_r (radial component of velocity), and V_θ (horizontal component of velocity). For the atmospheric flight phase, from point 2 to point 3 in Fig. 1, the equations of motion are as follows:

$$\frac{dr}{dt} = V_r \qquad \frac{d\theta}{dt} = \frac{V_\theta}{r}$$

$$\frac{dV_r}{dt} = -\frac{D}{m}\cdot\frac{V_r}{V} + \frac{L}{m}\cdot\frac{V_\theta}{V} - \frac{V_r V_\theta}{r}$$

$$\frac{dV_\theta}{dt} = -\frac{D}{m}\cdot\frac{V_\theta}{V} - \frac{L}{m}\cdot\frac{V_r}{V} + \frac{V_\theta^2}{r} - \frac{\mu}{r^2} \qquad (1)$$

where t is time; V is the magnitude $\sqrt{V_r^2 + V_\theta^2}$ of the velocity; m is the vehicle mass; and D and L are the aerodynamic drag and lift forces, respectively. The latter are given by the equations

$$D = \tfrac{1}{2}\rho(r)V^2 C_D A$$

$$L = \tfrac{1}{2}\rho(r)V^2 C_L A \qquad (2)$$

where C_D and C_L are the drag and lift coefficients, respectively, referenced to a nominal cross-sectional area A; and $\rho(r)$ is the atmospheric density. Most of the energy dissipation occurs in a limited range of altitudes, over which the density $\rho(r)$ varies approximately as $\exp(-r/H)$, the atmospheric scale height H being a constant.

Above a certain altitude r_0, the motion is essentially Keplerian. If the asymptotic approach velocity relative to the planet is V_∞, and if the asymptotic approach path passes the

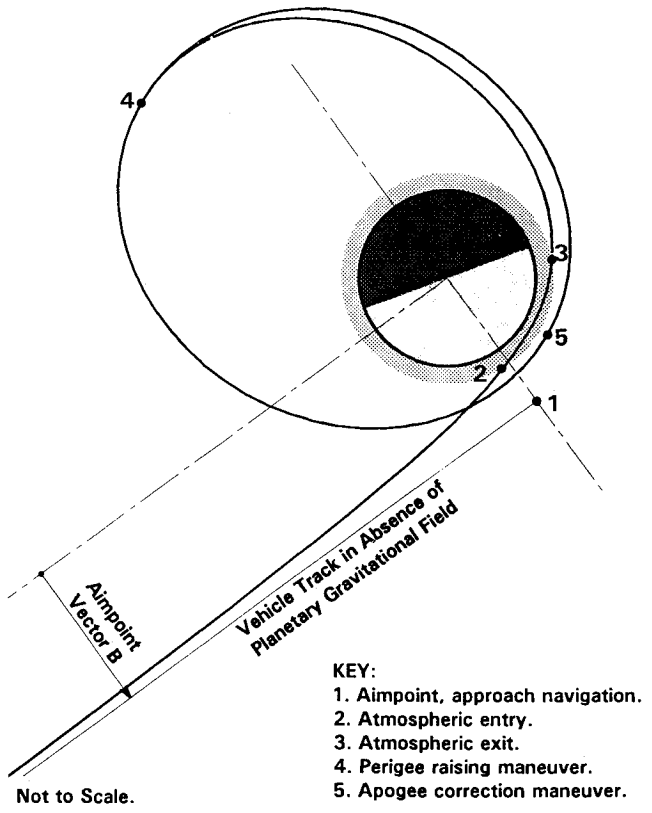

Fig. 1 Schematic of an aerocapture maneuver.

Received May 2, 1991; revision received July 20, 1992; accepted for publication Aug. 7, 1992.

*Chief Scientist, Systems Laboratories Directorate, Space and Communications Group; current address 10901 Savona Road, Los Angeles, CA 90077.

planet at a distance B from its center, then the initial conditions are

$$r = r_0$$

$$V_\theta = BV_\infty/r_0$$

$$V_r = -\sqrt{V_\infty^2 + 2\mu/r_0 - (BV_\infty/r_0)^2}$$

$$\theta = \cos^{-1}\left(\frac{1-p/r_0}{e}\right) - \cos^{-1}\left(\frac{1}{e}\right) \tag{3}$$

where p is the semilatus rectum $B^2V_\infty^2/\mu$ and e is the orbital eccentricity $\sqrt{1+pV_\infty^2/\mu}$.

On exit from the atmosphere, when the radius r exceeds r_0 with V_r positive, the apogee of the capture orbit, if capture has been achieved, is calculated by computing first the semilatus rectum p and the eccentricity e

$$p = r^2V_\theta^2/\mu$$

$$e = \sqrt{1-2p/r+pV^2/\mu} \tag{4}$$

where V is the magnitude $\sqrt{V_r^2+V_\theta^2}$ of the inertial velocity. If capture has been achieved, then e is less than unity, and the apogee radius has the value

$$r_a = p/(1-e) \tag{5}$$

Control of the vehicle's trajectory during the aerocapture maneuver is exercised through control of the aerodynamic coefficients C_D and C_L, usually by altering the angle of attack

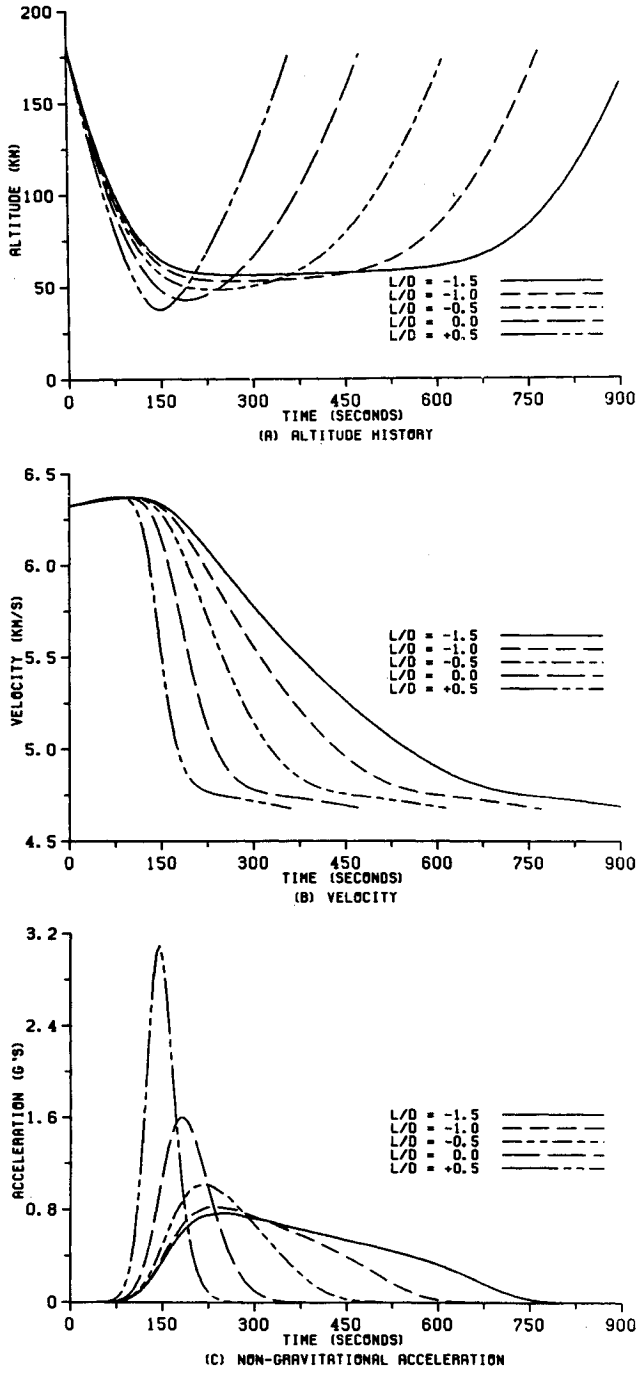

Fig. 2 Effects of varying lift-to-drag ratio.

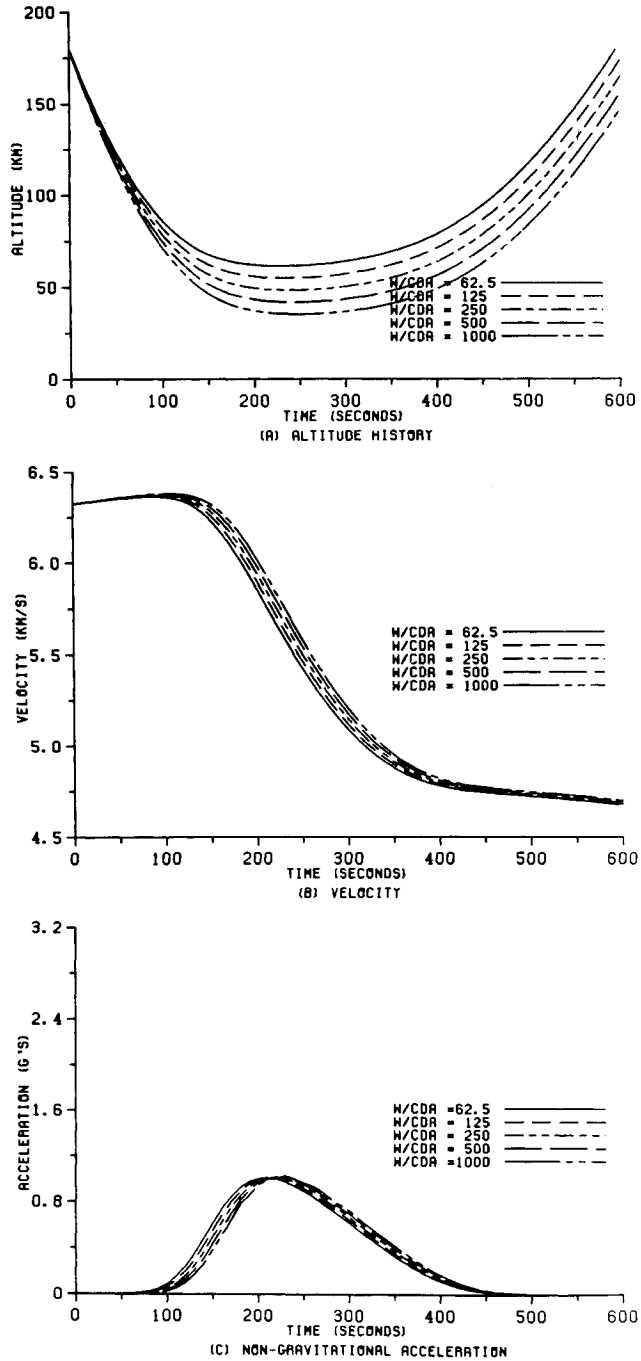

Fig. 3 Effects of varying ballistic coefficient.

α. This results in control of the value of the lift coefficient C_L within a limited range C_{L1} to C_{L2}. This may entail some variation in the drag coefficient C_D also; however, in the simplified model examined in this study, C_D was assumed fixed, independent of α and C_L.

We assume that, for nominal re-entry conditions, the vehicle holds a nearly constant angle of attack. In this case, the nominal trajectory depends on two vehicle parameters, the ballistic coefficient m/C_DA and the ratio L/D of lift to drag. Figures 2 and 3 show how these two parameters affect the capture trajectory. The example presented in these figures represents a vehicle approaching Mars with an asymptotic speed of 4 km/s (corresponding to a near-minimum-energy transit from Earth), captured into an orbit having an apogee altitude of 37,200 km. With this apogee, and a subsequent maneuver to raise the perigee altitude to about 250 km, above most of the atmosphere, one will attain a highly elliptical Mars-synchronous orbit (period 1 sol, or 1 Martian day). The perigee raising maneuver requires a propulsive velocity impulse of about 30–40 m/s, applied near apogee.

Figure 2 exhibits the qualitative differences between low (or positive) L/D and highly negative L/D trajectories. Low L/D trajectories involve relatively steep flight-path angles at entry and exit and relatively short time spent in the atmosphere; the minimum altitude reached is relatively low and the peak deceleration relatively high. Using high negative L/D, one extends the time duration of the aerobraking maneuver, resulting in shallower flight-path angles at entry and exit, higher minimum altitude, and lower peak deceleration.

Figure 3 shows that, as the ballistic coefficient varies, the shape of the time history curves is essentially unchanged, except for a vertical offset in altitude and a small time delay associated with the variable time from crossing the reference altitude level of 180 km, until reaching a particular density level.

Table 1 shows how impractical it would be to attempt an aerocapture maneuver relying exclusively on open-loop attitude control. Too shallow an entry or too much lift (or insufficient negative lift) and the spacecraft will not be captured or will leave the atmosphere with an orbital period which is excessively large. Too steep an entry, and the spacecraft velocity may become suborbital, resulting in an unintended re-entry and possible destruction due to excessive aerodynamic forces or thermal loads. For moderate values of negative L/D, the accuracy of the aimpoint offset B required to achieve an apogee altitude within ± 200 km of the target value, is only a few millimeters. This far exceeds any reasonable approach guidance accuracy and is several orders of magnitude smaller than the uncertainties in B caused by imperfect knowledge of vehicle aerodynamic coefficients, atmospheric density profile, and winds.

Table 1 Tolerance on aimpoint offset distance B, m[a]

L/D	Apogee = 37,400 km, B_1	Apogee = 37,000 km, B_2	Tolerance $(B_1 - B_2)/2$
−1.5	72286.555	72286.553	0.001
−1.0	68200.161	68200.105	0.028
−0.5	61606.230	61605.075	0.578
0.0	48430.976	48417.416	6.780
+0.5	20390.982	20318.916	36.033

[a]Columns 2 and 3 give incremental values relative to a trajectory which, in the absence of atmospheric forces, would just graze the surface of Mars.

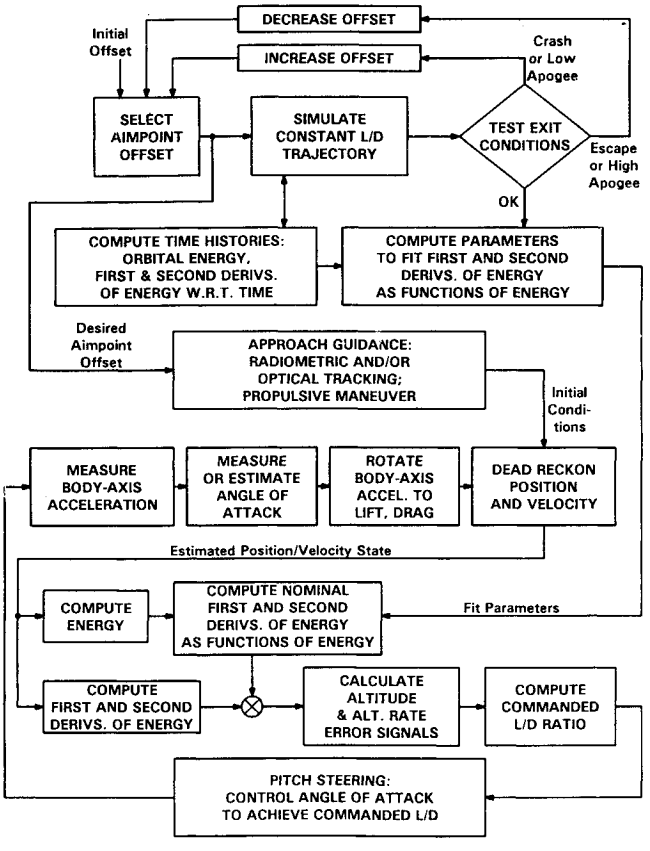

Fig. 4 Navigation and guidance data flow.

III. Description of the Guidance Law

The guidance concept discussed here is designed to avoid large variations in the apogee altitude of the capture orbit associated with reasonable dispersion in initial conditions, arrival time, and knowledge of the atmospheric density profile. The guidance law is based on controlling the rate of dissipation of total orbital energy until there is just enough energy left to achieve the desired apogee of the final orbit. This is similar to the energy controller concept of Gamble et al.,[4] except that a precomputed nominal trajectory is used to provide positive control of the aerobraking maneuver time profile.

The guidance computations involve three stages (Fig. 4). First, a nominal entry trajectory is established, following a selected lift-to-drag profile. The aimpoint used for approach navigation is selected so as to achieve a postcapture orbit with the desired apogee radius. The second stage involves approximating the first-order and second-order time derivatives of the orbital energy $V^2/2 - \mu/r$ as functions of energy. These two stages of the computation can both be precomputed before beginning the maneuver. The third state of computation, representing the realtime operational guidance, generates the pitch steering commands required to follow this precomputed energy profile.

The instrumentation required to implement this guidance scheme consists of a source of tracking data to characterize the approach trajectory, inertial instrumentation to sense the axial and normal components of the aerodynamic acceleration, and instrumentation or test data concerning the angle of attack, which is needed to compute the drag and lift forces from the body-axis forces. From these inputs, one can dead reckon the current trajectory state and derive pitch commands to control the aerocapture maneuver through adjustment of the angle of attack.

During the atmospheric phase of the mission, while the dynamic pressure is sufficient for effective aerodynamic control, the lift-to-drag ratio is controlled by pitch steering, so that the rate of dissipation of orbital energy matches the desired rate based on the precomputed nominal trajectory. Expressed in terms of the state variables and the drag acceleration D/m, the

present total orbital energy, the rate of energy dissipation, and the second derivative of total energy are given by

$$E = -\mu/r + V^2/2$$

$$\dot{E} = -VD/m$$

$$\ddot{E} = -\left[(3g/V^2 + 1/H)\cdot V_r + 3VD/m\right]\cdot \dot{E} \qquad (6)$$

where g is the gravitational acceleration μ/r^2. In the onboard guidance computer, the present energy E, the initial energy $E_0 = V_\infty^2/2$, and the target orbital energy

$$E_{\text{tgt}} = -\mu/(r_p + r_a) = -\mu/\left[p/(1+e) + r_a\right] \qquad (7)$$

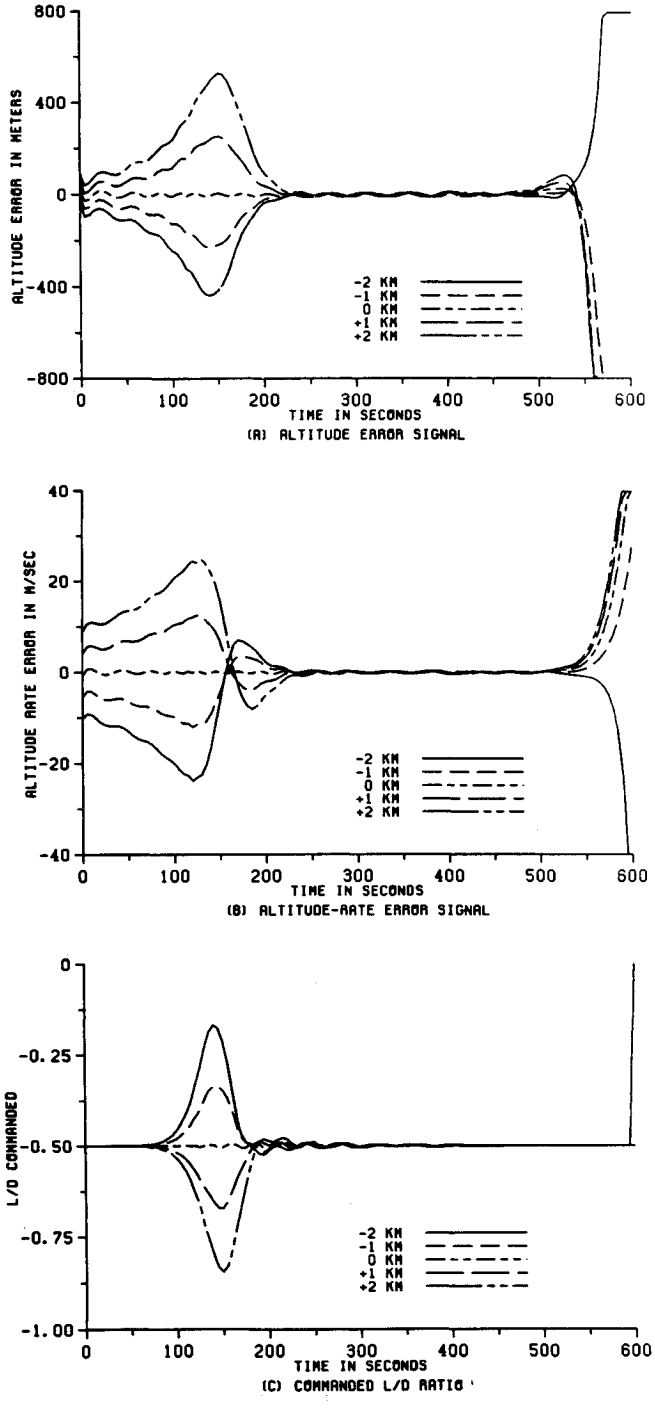

Fig. 5 Steering out aimpoint offsets.

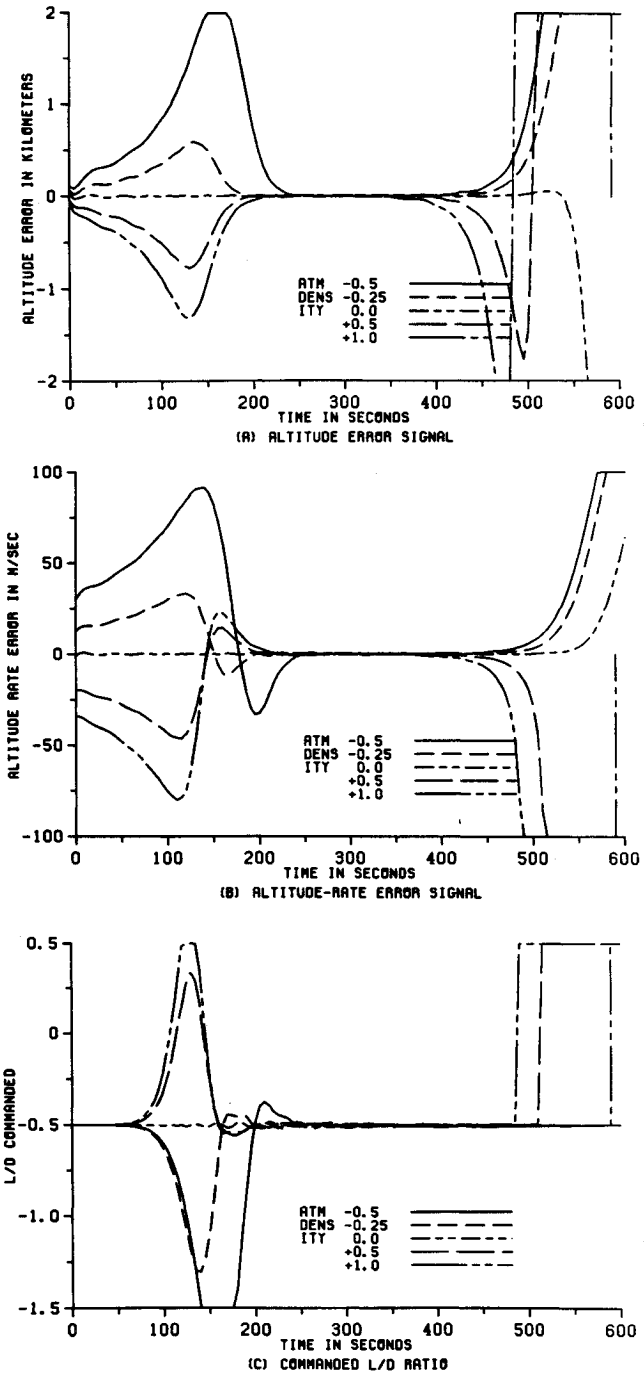

Fig. 6 Response to off-nominal atmospheric density.

needed to achieve the desired apogee radius r_a, are combined in a dimensionless function of orbital energy,

$$\phi = \frac{E_0 + E_{\text{tgt}} - 2E}{E_0 - E_{\text{tgt}}} \qquad (8)$$

which serves as a measure of how far the aerocapture maneuver has progressed, from atmospheric entry ($\phi = -1$) to exit on the desired capture orbit ($\phi = +1$). Using ϕ as an argument, the guidance computer determines the values $F_1(\phi)$ and $F_2(\phi)$ which two "control functions"

$$S_1 = \frac{-(E_0 - E_{\text{tgt}})\dot{E}}{(E_0 - E)(E - E_{\text{tgt}})} = \frac{(E_0 - E_{\text{tgt}})VD/m}{(E_0 - E)(E - E_{\text{tgt}})}$$

$$S_2 = -\frac{\ddot{E}}{\dot{E}} = \left(\frac{3g}{V^2} + \frac{1}{H}\right)\cdot V_r + \frac{3D/m}{V} \qquad (9)$$

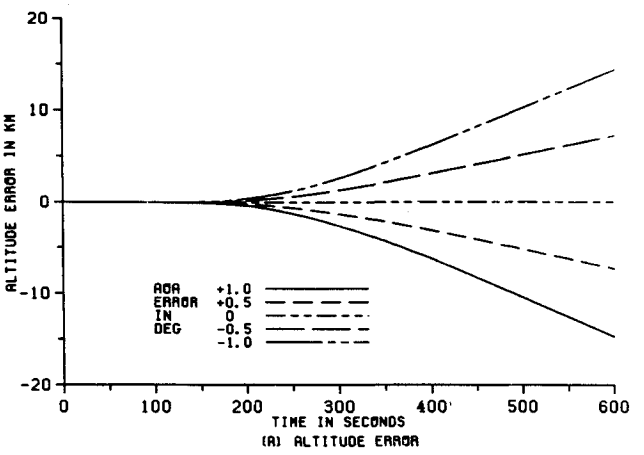

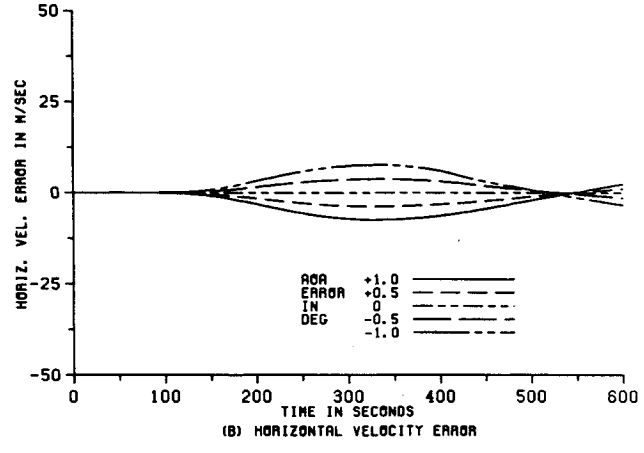

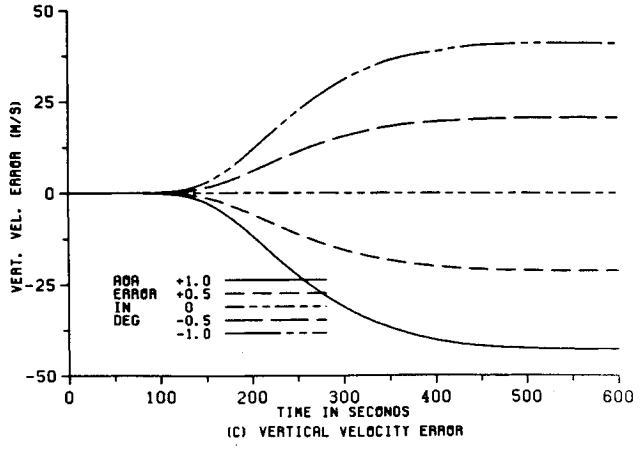

Fig. 7 Navigation errors caused by error in angle of attack.

would have, if the vehicle were following the prescribed nominal trajectory. Discrepencies between these nominal-trajectory values and values computed from the dead-reckoned position and velocity and the measured drag acceleration are indicative of the discrepancies between the actual and nominal altitude and altitude rate Δh and $\Delta \dot{h}$.

$$S_1 = F_1(\phi) + \Delta h \frac{\partial S_1}{\partial r} + \Delta \dot{h} \frac{\partial S_1}{\partial V_r}$$

$$S_2 = F_2(\phi) + \Delta h \frac{\partial S_2}{\partial r} + \Delta \dot{h} \frac{\partial S_2}{\partial V_r} \tag{10}$$

where the partial derivatives, with ϕ (or energy E) held constant, are

$$\frac{\partial S_1}{\partial r} = -S_1\left(\frac{1}{H} + \frac{3g}{V^2}\right)$$

$$\frac{\partial S_1}{\partial V_r} = 0$$

$$\frac{\partial S_2}{\partial r} = -\frac{3D/m}{V}\left(\frac{1}{H} + \frac{g}{V^2}\right) + \frac{6g^2}{V^4} V_r$$

$$\frac{\partial S_2}{\partial V_r} = \frac{1}{H} + \frac{3g}{V^2} \tag{11}$$

The final step is to command a lift-to-drag ratio L/D which, if Δh and $\Delta \dot{h}$ are both zero, will match the value for the nominal trajectory $(L/D)_0$, but for nonzero Δh and $\Delta \dot{h}$ has additive terms proportional to each

$$L/D = (L/D)_0 - G_v \Delta \dot{h} - G_r \Delta h \tag{12}$$

In effect, a linear combination of altitude and altitude rate deviations is used to control the lift-to-drag ratio and hence the vertical acceleration.

Since control authority is present only when the dynamic pressure is sufficient to exert significant lift forces, it was found expedient to program the control loop gain to be proportional to the nominal atmospheric density. This results in a gradual buildup of commanded lift-to-drag ratio in response to small initial guidance errors. In some cases, the residual error on exiting the atmosphere was large enough to saturate the control loop, although in some runs where this occurred the parameters of the capture orbit were reasonably close to those of the target orbit.

One of the advantages of this guidance scheme is that the control of energy dissipation rate is essentially equivalent to controlling the density altitude, providing partial compensation for deviations from the nominal atmospheric density profile. Similarly, the dead reckoning of energy dissipation rate also provides compensation for off-nominal aerodynamics of the vehicle and for variability in winds.

IV. Simulation Results

The guidance scheme shown in Fig. 4 has been used to simulate the case of a vehicle approaching Mars with an asymptotic velocity of 4.0 km/s, captured into a highly elliptical orbit with a period of 1 sol (1 Martian day). Perigee altitude is 250 km and apogee radius is 37,200 km.

The guidance law was able to follow the prescribed nominal flight profile over the range of L/D values tested, from -1.5 to $+0.5$, and for various values of the ballistic coefficient from 62.5 to 1000 kg/m^2. The control law has good stability and is sufficiently accurate to achieve capture with an apogee radius within a few tens of meters of the target radius of 37,200 km.

Next, the guidance law was exercised to test the stability and accuracy of the control by examining the pitch steering response to off-nominal approach conditions and off-nominal atmospheric parameters. Figure 5 presents the results of a series of runs showing the ability of the guidance law to adjust for variations in the initial aimpoint. After generating a nominal constant L/D entry trajectory (the $L/D = -0.5$ trajectory of Fig. 2), we offset the approach trajectory aimpoint displacement B (the miss distance for a hypothetical zero-mass planet) by various amounts, from -2 km (2 km closer to the planet) to $+2$ km (2 km farther out). Figures 5a and 5b show the resulting indicated altitude rate error and altitude error, respectively, based on measurements of position and velocity which give perfect knowledge of total energy and perigee altitude and perfect measurement of aerodynamic forces. Figure

5c shows the lift-to-drag ratio commanded in response to these altitude and altitude rate errors.

Control signals representing altitude error and altitude rate error build up gradually as the vehicle enters the sensible atmosphere, but the commanded lift-to-drag ratio remains at the nominal value until the atmospheric density is sufficient to provide effective control. This is achieved by programming the control gain as a function of atmospheric density.

The apogee altitude reached after exiting from the atmosphere is within a few kilometers of the targeted apogee altitude. The control scheme represented is successful in achieving capture into an orbit which closely approximates the parameters of the target orbit, in spite of significant variability in initial entry conditions.

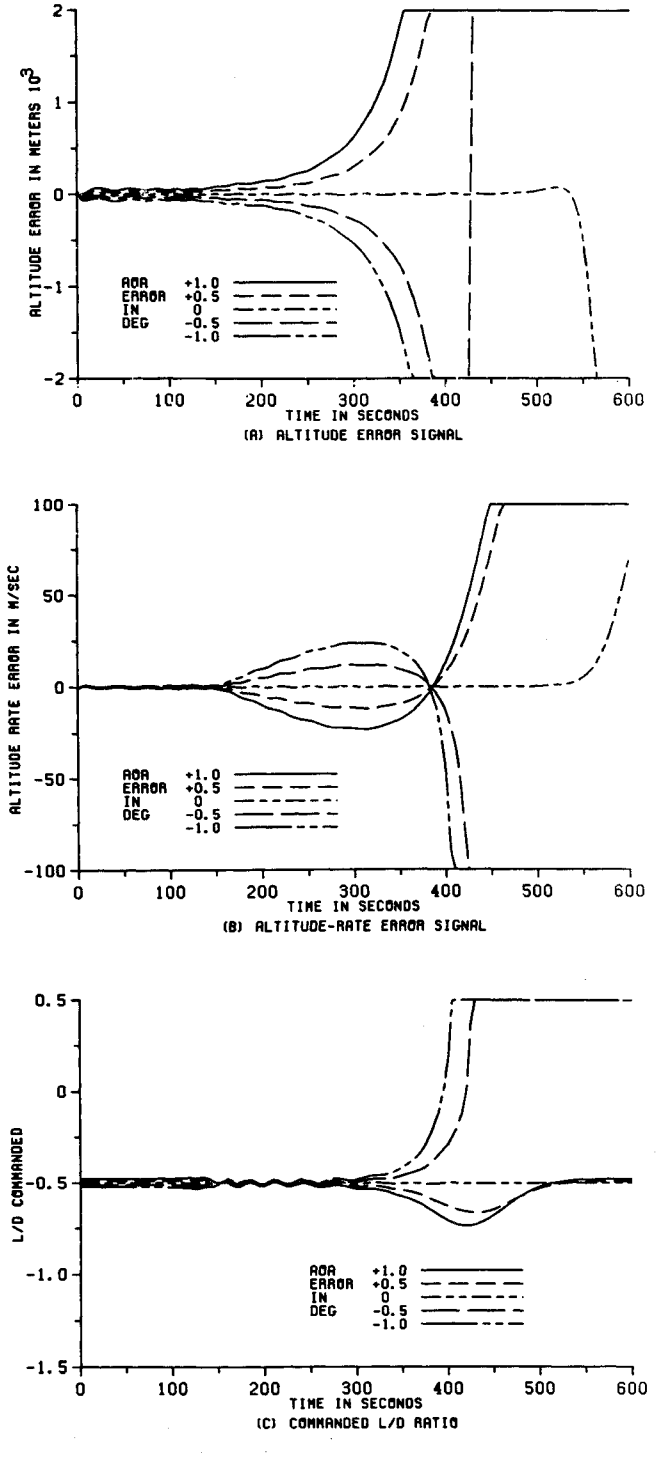

Fig. 8 Guidance response to angle-of-attack errors.

Table 2 Effects of angle-of-attack errors

Error in AOA, deg	Apogee radius, km
−1.0	49,186.6
−0.5	42,183.1
0.0	37,200.4
+0.5	33,622.4
+1.0	30,981.1

In Fig. 6 we see the response to off-nominal atmospheric density. Variations up to −50% or +100% are accommodated, with only moderate residual errors in apogee altitude (under 200 km).

V. Robustness of the Control

The preceding results show that we can define a nominal constant L/D aerocapture trajectory, and control the vehicle to achieve capture into the specified orbit for a reasonable spread of approach trajectory parameters. The next question to address concerns the ability of the control system to function properly when the knowledge of the trajectory state and the aerodynamic force model is imperfect.

Imperfect navigation can cause serious errors in the parameters of the capture orbit. For a guidance system with measurements of body-axis nongravitational acceleration only, such errors arise because of inaccurate approach navigation, imperfect modeling of gravitational forces, accelerometer errors such as bias or scale factor, and inaccurate estimation of the angle of attack, used to resolve the body-axis acceleration components into lift and drag. For reasonable instrument performance, this last source of error is likely to dominate.

Figure 7 shows the effect on navigation error of error in estimation of angle of attack, for errors up to ±1.0 deg. Figure 8 shows the resulting guidance response. Apogee altitude errors on the order of 10,000 km are incurred (Table 2) for an angle-of-attack error of 1 deg. However, since the navigation errors are primarily errors in altitude and altitude rate (Figs. 7a and 7c, respectively), a radar altimeter would provide good instrumentation for detection and correction of this error.

VI. Conclusions

Negative-lift aerocapture trajectories are preferable to zero or positive-lift trajectories because they result in lower peak acceleration and higher minimum altitudes. But they also result in extremely narrow safe-capture corridors, which presents a severe guidance and control problem. The guidance scheme described here provides a closed-loop control to force the vehicle to follow a preplanned path through this corridor. The primary input is the measured drag acceleration, obtained by resolving the sensed body-axis acceleration components through the angle of attack. The critical instrumentation requirement is judged to be that for angle of attack. Angle-of-attack errors of 0.5–1.0 deg are shown to yield dispersions of the capture orbit apogee altitude which are undesirably large. Alternative instrumentation, such as an inertial navigation quality pitch-axis gyroscope or a radar altimeter for direct sensing of vertical velocity, is indicated.

References

[1]Anon., "Report of the 90 Day Study on Human Exploration of the Moon and Mars," NASA Internal Document, Nov. 20, 1989.

[2]Woodcock, G. R., and Sherwood, B., "Engineering Aerobrakes for Exploration Missions," AIAA Paper 89-0213, Jan. 1989.

[3]Gamber, R., and Rogers, L., "Aerocapture, Entry and Landing for the Mars Rover Sample Return Mission," AIAA Paper 89-0422, Jan. 1989.

[4]Gamble, J. D., Cerimele, C. J., Moore, T. E., and Higgins, J., "Atmospheric Guidance Concepts for an Aeroassist Flight Experiment," *Journal of the Astronautical Sciences,* Vol. 36, Jan.–June 1988, pp. 45–71.